of weathered chances zones within hydrological soil group 'D' having poor infiltration rate and run-off (> 130 mm) with a slope of > 15% in the village of A. Vellodu and Dindigul town.

1. Rangarajan, R. and Athavale, R. N., Annual replenishable groundwater potential of India – an estimate based on injected tritium studies. *J. Hydrol.*, 2000, **234**, 38–53.
2. Muralidharan, D. and Shanker, G. B. K., Various methodologies of artificial recharge for sustainable groundwater in quantity and quality for developing water supply schemes. Proceedings of the All Indian Seminar on Water Vision for the 21st Century, IAH, Jadavpur University, Kolkata, 2000, pp. 208–229.
3. Mondal, N. C. and Singh, V. S., Aquifer modelling study in and around Dindigul town, Tamil Nadu, India. In *Proceedings of the International Conferance (WE-2003, Bhopal) on Water and Environment, Ground Water Pollution* (eds Singh and Yadava), Allied Publishers Pvt. Ltd., 2003, pp. 188–198.
4. Mondal, N. C. and Singh, V. S., Hydrogeological, geophysical and hydrochemical studies for delineating groundwater contamination zones in the tannery belt, Tamil Nadu, India. In *Proceedings. of the International Conferance (WE-2003, Bhopal) on Water and Environment, Ground Water Pollution* (eds Singh and Yadava), Allied Publishers Pvt. Ltd., 2003, pp. 262–277.
5. Public Works Department, Groundwater perspectives: a profile of Dindigul District, Tamil Nadu. Report, PWD, Govt. of India, Chennai, 2000, p. 78.
6. Balasubrahmanian, K., Geology of parts of Vedasandur Taluk, Madurai District, Tamil Nadu. Progress Report, GSI Tech. Rep. Madras, 1980, p. 14.
7. Chakrapani, R. and Manickyan, P. M., Groundwater resources and developmental potential of Anna District, Tamil Nadu State. CGWB, Report, Southern Region, Hyderabad, 1988, p. 49.
8. Krishnan, M. S., *Geology of India and Burma*, CBS Publishers and Distributions, India, 1982.
9. Thangarajan, M. and Singh, V. S., Estimation of parameters of an extensive aquifer – a case study. *J. Geol. Soc. India*, 1998, **52**, 477–481.
10. Athavale, R. N., Murti, C. S. and Chand, R., Estimation of recharge to the phreiatic aquifers of Lower Maner Basin, India by using the tritium injection method. *J. Hydrol.*, 1980, **45**, 185–202.
11. Athavale, R. N., Chand, R., Murali, D. M., Muralidharan, D. and Murthy, C. S., Measurement of groundwater recharge in Marvanka basin, Anantapur district. In Int. Proc. of a Seminar on Assessment of Groundwater Resources, CGWB, New Delhi, 1983, vol. III, pp. 275–290.
12. Rangaranjan, R., Deshmukh, S. D., Prasad Rao, N. T. V. and Athavale, R. N., Natural recharge measurements in Upper Hanti watershed in Jhabua district, Madhya Pradesh, Tech. Report. No. NGRI-95-GW-183, 1995, p. 24.
13. Rangarajan, R., Natural recharge evaluation in selected basins of semi-arid India using injected tritium method. Ph D thesis, Osmania University, Hyderabad, 1997, p. 180.
14. Grewal, B. S., *Higher Engineering Mathematics*, Khanna Publisher, Delhi, 1993, p. 1224.

ACKNOWLEDGEMENTS. We thank Dr V. P. Dimri, Director, NGRI for permission to publish this paper and PWD and IRS, Anna University, Chennai for providing data. N.C.M. thanks CSIR, New Delhi for partial financial support to carry out this work. Mr Verghese is acknowledged for preparation of the manuscript. We also thank the anonymous reviewer for his valuable suggestions.

Received 6 March 2004; revised accepted 25 May 2004

Concentric rings of radioactive halo in chlorite, Turamdih uranium deposit, Singhbhum Shear Zone, Eastern India: a possible result of ^{238}U chain decay

Dipak C. Pal

Department of Geological Sciences, Jadavpur University, Kolkata 700 032, India

Transmitted light microscopy of quartz-chlorite schist from Turamdih uranium deposit in Singhbhum Shear Zone has revealed the presence of distinctly circular aureoles of radiation damage, commonly referred to as radioactive halos or radiohalos, in chlorite surrounding inclusions of uraninite in the Turamdih uranium ore; particularly those surrounding tiny (< 2 μm) radiocentres show spectacular concentric aureoles. In well-developed halos, four distinct rings of discoloration are clearly visible in host chlorite. The radiohalo pattern is in good agreement with the theoretical radiohalo pattern of ^{238}U based on α-penetration ranges in air. Radii of individual rings surrounding tiny radiocentres (< 2 μm) in diametral/near-diametral sections are consistent and the mean radii of 32.4 μm (outermost), 22.0, 18.3 and 15.2 μm (innermost) compare well with the experimentally determined, theoretically calculated and observed penetration depths of α-particles emitted by ^{214}Po (the outermost ring), ^{218}Po, ^{210}Po/^{222}Rn, and ^{226}Ra/^{234}U/^{230}Th (innermost ring) in biotite. Such ring structures can be assigned to the decay chain of ^{238}U in which the above radioactive atoms correspond to daughters in the decay series and each of them emits α-particles of different energies. The undeformed circular nature of the radiohalos is indicative of their post-kinematic origin. Petrographic studies also indicate possible mobilization of uranium by some later processes.

IN some minerals, notably biotite, fluorite, chlorite, cordierite, etc. tiny aureoles of discoloration, commonly referred to as radioactive halo or radiohalo are found and in many instances such aureoles are characterized (on microscopic examination) by concentric dark and light rings surrounding a central radioactive inclusion. The causes of such discoloration of minerals are commonly assigned to radiation damage. Understanding radiation damage in synthetic and natural samples is extremely important, particularly in relation to the containment of radioactive wastes. Sheet silicates and clays are common minerals found in a variety of rocks and are common constituents in engineered-barriers in high-level nuclear waste site. These minerals can significantly reduce the migration of radionuclides[1] through groundwater by adsorbing them on the surface or incorporating some of the elements at inter-layer sites.

e-mail: dcpaly2k@yahoo.com

However, such properties of these minerals may be lost by long-term radiation-induced amorphization[1]. Understanding radiation damage in sheet silicates and clays is therefore critical to assess long-term repository behaviour. Studying natural samples is one of the best ways to understand long-term radiation effects. Amongst the sheet silicates, radiohalo patterns, penetration depths of α and nature of damage in natural samples have possibly been best documented in case of biotite[2–6]. Although chlorite has the potential to record radiohalos similar to biotite, such studies, particularly in natural samples, are virtually lacking possibly because of non-availability of reported and well-documented radiohalos in chlorite. Petrographic characterization of radiation damages forms the foundation of any detailed study using modern techniques. The objective of the present study is to identify the radiohalo pattern and quantify the aureoles of radiation damages in chlorites surrounding uraninite from Turamdih and compare them with available data on a sheet silicate like biotite.

Radiation damage in minerals is caused mainly by α-emission from radioelements, although contribution from β-emission has also been advocated[7]. α-particles cause damage in crystal lattice mainly[8] (a) by ionizing atoms along their path, (b) by knocking-off atoms producing interstitial atoms and vacancies, known as Frenkel pairs, and (c) by producing very high temperature for a very short period of time along their path and causing thermal damage. Metamictization, particularly of zircon, is one of the most commonly studied types of radiation damage and recent investigations suggest that long-term accumulation of damages by α-decay events causes transformation of initial crystalline material to amorphous state of metamict minerals[9–11]. Such damages are caused dominantly by recoil of heavy daughter nuclei on emission of α-particles, and contributions of other processes like ionization, formation of point defects and spontaneous fission are negligible[12,13]. Radiohalos, on the other hand, are possibly the result of short-term accumulation of damages[4]. In a comprehensive study, Nasdala *et al.*[4] have shown that ionization by α-particles produces a *sphere* of radiation, which appears as a *full circle* in thin sections surrounding radiation source. On the contrary, *spherical shell* of radiation damage that appears as *concentric ring* in thin sections (not as full circles) and commonly found in natural biotites[2], is generated by atomic displacements producing Frenkel pairs at the end of the path of α-particles. The penetration depths of α-particles and hence the radius of ring/circle is dependent on the energies of α-particles and the nature of the medium through which they penetrate[2–4]. Since a particular radioactive atom emits α-particles with specific characteristic energy, the radius is characteristic of a particular radionuclide in a given medium. Consequently, if a radiocentre contains a radionuclide that produces a decay series, a group of concentric rings/circles is possible provided none of the α-emitters in the series leaves the system before producing discernible damage. The radius of each ring will correspond in such a case to a step in the decay series. ^{238}U is one of such radionuclides and it decays through eight alpha-decay steps (Table 1). The α-emitters in the decay chain of ^{238}U are ^{238}U, ^{234}U, ^{230}Th, ^{226}Ra, ^{222}Rn, ^{218}Po, ^{214}Po and ^{210}Po. Accordingly, eight concentric rings are expected in well-developed radiohalos. However, as shown in Table 1, the energies of α particles in air (E_α) emitted by ^{234}U, ^{230}Th and ^{226}Ra are very close. Similarly, E_α for ^{222}Rn is close to that of ^{210}Po. Consequently, characteristic rings of ^{234}U, ^{230}Th and ^{226}Ra and those of ^{222}Rn and ^{210}Po cannot be distinguished in the resolution of common transmitted light microscope. Thus on microscopic examination, five distinct rings corresponding to ^{214}Po, ^{218}Po, ^{222}Rn/^{210}Po, ^{234}U/^{226}Rn/^{230}Th and ^{238}U are often visible in well-developed radiohalos. Best ring structures are developed when the radiocentre is extremely small in size. Larger radiocentres generally develop poor ring structure, partly because of overlapping thick shells/spheres produced by alphas emitted from the centre as well as those from the boundary of radioactive inclusion.

Singhbhum Shear Zone, extended over a length of approximately 200 km, is one of the most important economic belts in India and is well known for its rich mineralization of U and Cu and other base and noble metals as by-products. Uranium and copper mineralization in Turamdih is hosted by occasionally feldspathized quartz-chlorite

Table 1. α-decay events, reported penetration depths of α in biotite and mean ring radius (penetration depth) observed in the present study

α-decay event	α-energy (E_α) in MeV[@]	Penetration depth in biotite (μm): ^{4}He-induced coloration bands[#] (μm)	Observed radius[#] (μm)	Monte Carlo simulation[$] (μm)	Mean radius of damaged aureoles in chlorite (this study; μm)
^{238}U → ^{234}Th	4.198	13.4–13.8	12.2–13.0	13.5	
^{234}U → ^{230}Th	4.775	16.7	14.9–15.6	16.2	
^{230}Th → ^{226}Ra	4.688	–	NR	15.7	15.2
^{226}Ra → ^{222}Rn	4.784	16.7	14.9–15.6	16.2	
^{222}Rn → ^{218}Po	5.489	20.5	17.9–18.8	19.7	
^{218}Po → ^{214}Pb	6.022	23.0	21.7–22.2	22.5	22.0
^{214}Po → ^{210}Pb	7.687	33.1–33.9	31.0–32.9	32.7	32.4
^{210}Po → ^{206}Pb	5.304	19.3	NR	18.8	18.3

[@]After Firestone and Shirley[15]; [#]After Gentry[2]; [$]After Nasdala *et al.*[4].

schist containing variable proportions of muscovite and biotite. Tiny but discrete grains of uraninite are concentrated mostly in chlorites. Chalcopyrite, pyrite, magnetite and ilmenite are the other ore minerals. Sarkar[14] observed concentric zones of intense absorption of light in host mineral surrounding uraninite from Singhbhum Shear Zone. However, detailed characterization of such halos and correlating them with specific α-emitters are lacking. In the present case radiohalos were studied under transmitted light microscope in thin polished sections (≈ 30 μm thickness) of rock samples collected from the underground mines at Turamdih. Radiation damages are noted surrounding uraninite and also some silicates (epidote). However, the present study is restricted mainly to the radiohalos surrounding uraninite in chlorite of the host rock. Figure 1 *a* shows the overall view of radiohalos observed in chlorite surrounding uraninite. Radiohalos surrounding silicates (epidote) are characterized by even discoloration and concentric rings are absent (Figure 1 *b*). This may be due to the comparatively much larger size of silicate inclusions producing overlapping zones of damaged shells. However, the presence or absence of concentric rings is also dependent on the nature of radionuclide(s) present in the radiocentre and also on the nature of radiation damage (ionization vs atom displacement).

Uraninites in Turamdih are commonly equant in shape and the long axis rarely exceeds 10 μm. Such small size of uraninites inhibits detailed study of these grains under reflected light microscope. However, they are identified by brownish-grey colour, very low reflectivity (slightly less than that of magnetite) and isotropic nature. In oil medium, the reflectivity of uraninite falls and the reflectivity contrast between magnetite and uraninite is enhanced. Radiohalos surrounding tiny inclusions are generally less intensely coloured and display spectacular ring structures defined by alternate dark and light bands. On the contrary,

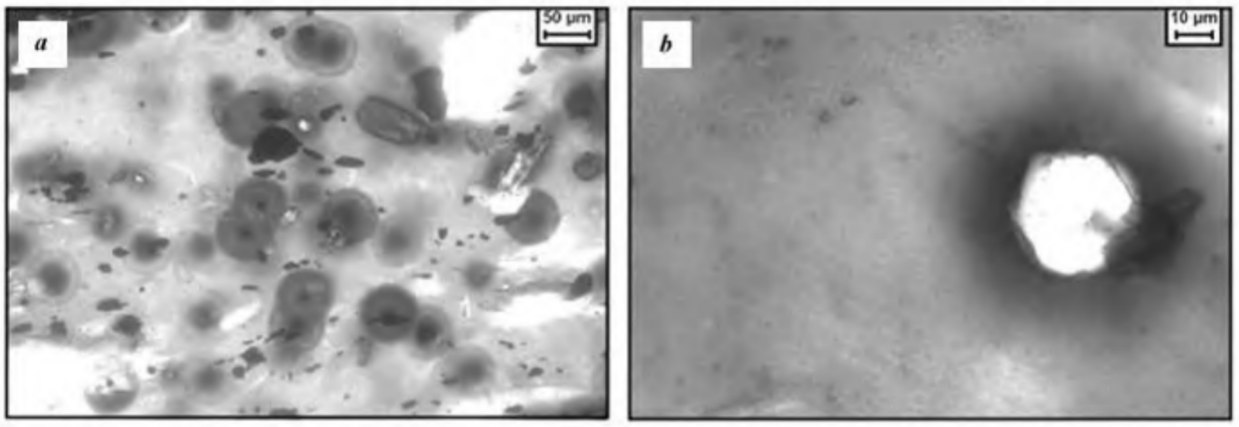

Figure 1. ***a***, Photomicrograph of generalized view of circular radiohalos in chlorite surrounding uraninite from Turamdih uranium deposit. The greyish mass is chlorite and the white patches on the top right and bottom left are quartz. Photograph taken under plane polarized light. ***b***, Photomicrograph showing even discoloration of chlorite surrounding radioactive silicate (epidote).

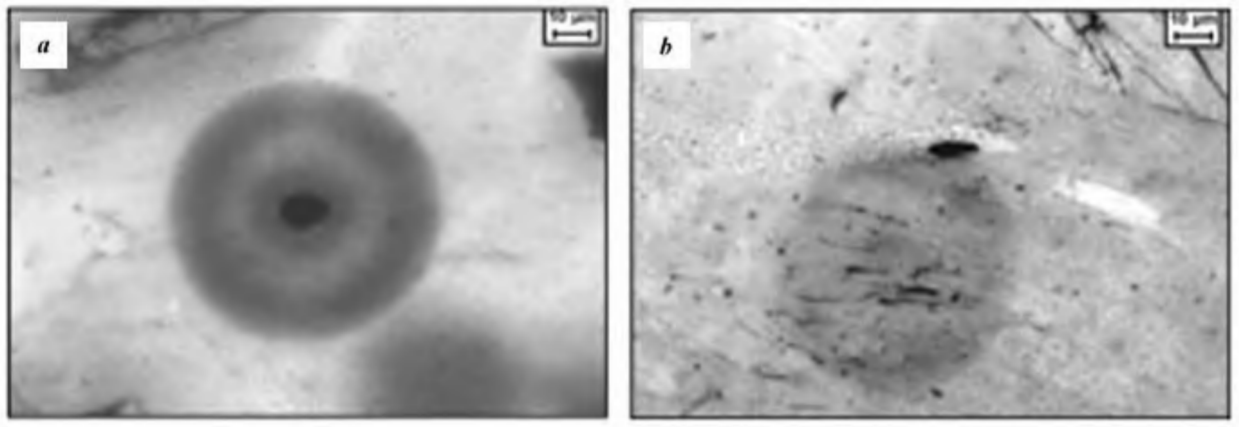

Figure 2. ***a***, Photomicrograph showing large radioactive halo in chlorite surrounding a large uraninite inclusion. The radius of the outermost halo of damaged aureole is 38.7 μm and the inclusion diameter is approximately 13.7 μm. ***b***, Photomicrograph showing homogenous discoloration. Note the absence of the radiocentre and also the presence of micro-fractures filled with unidentified dark minerals.

radiohalos surrounding large inclusions are more intensely coloured and the concentric rings are rarely discernible (similar to those found surrounding silicates). The aureoles of discoloration are also much larger in case of large inclusion producing some gigantic halos (Figure 2 *a*). In some cases the halo is characterized by homogenous discoloration of chlorite and this is particularly the case where the central radioactive inclusion is missing. The absence of radiocentres may be due to (i) the section not being a diametral one (passing through the centre of the spherical shell and hence through the radiocentre) or (ii) the radiocentre having been leached-off, particularly where the halo is closely associated with micro-fracture (Figure 2 *b*). It is to be noted that the radius of these halos in many cases is comparable with the maximum radius of the damaged aureoles in chlorite observed in the present study. Considering that the average thickness of the prepared thin sections is 30 μm and that the maximum radius of damaged aureole is generally 30–35 μm, it is difficult to explain the absence of the radiocentres on the basis of the non-diametral section. Hence, leaching-off of uranium by some later processes seems to be more plausible. If mobilization of uranium by later processes is pervasive, precaution should be taken while using U–Pb geochronological methods in deciphering the age of uranium mineralization. In some cases, concentric halos line up along the foliation planes (Figure 3 *a*), possibly indicating entry of radiocentres along the available favourable locales. Similar trails of haloed uraninite in mylonitic quartz-chlorite rocks from Jaduguda are also reported by Sarkar[14]. The circular radiohalos are truncated and disturbed at places by late quartz (Figure 3 *b*) and muscovite (Figure 3 *c*). Interestingly, in muscovite/sericite-rich samples radiohalos and the corresponding radiocentres are few. Even in a single sample, where muscovite/sericite replaces chlorite, the radiohalos are indistinct and the radiocentres are absent in many cases. This probably suggests that during the process of sericitization and silicification (possibly by late hydrothermal fluid), the radiocentres were selectively leached. This microscopic

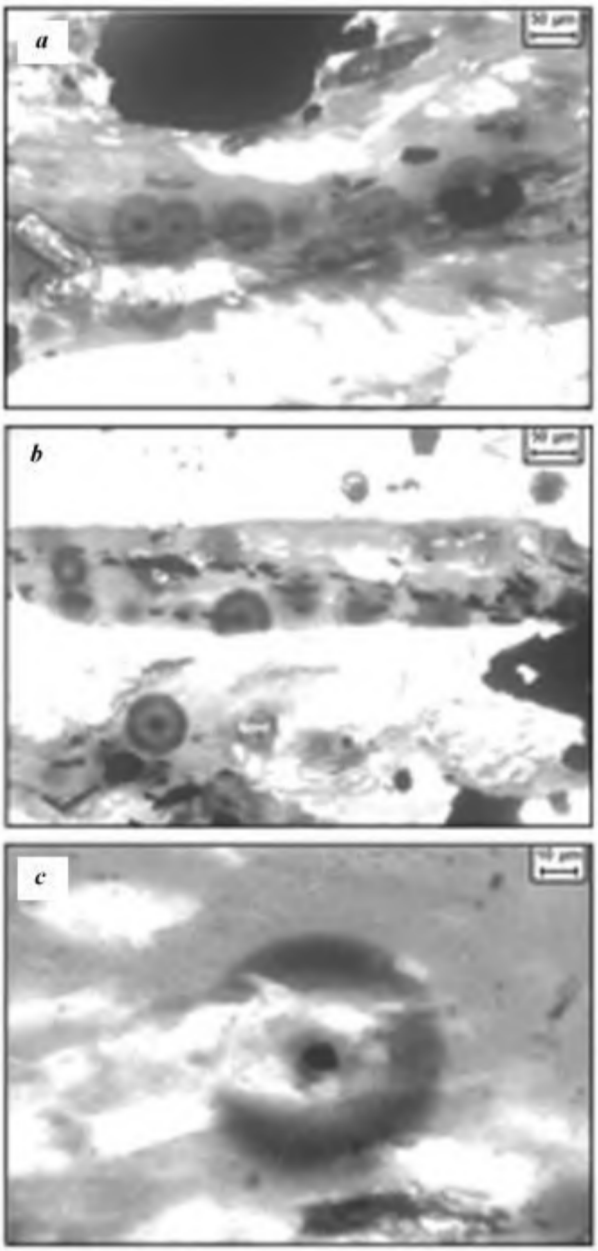

Figure 3. ***a***, Photomicrograph of trails of haloed uraninite paralleling the overall schistosity of quartz-chlorite schist. The schistosity runs nearly east-west. ***b***, Photomicrograph showing truncation of circular radioactive halo by late-quartz. At least three halos are clearly dissected by this quartz (colourless). Note the concentration of radiohalos in chlorite-rich part. ***c***, Photomicrograph showing replacement of chlorite (greyish) by sericite (white), partially destroying the radiohalo ring surrounding uraninite.

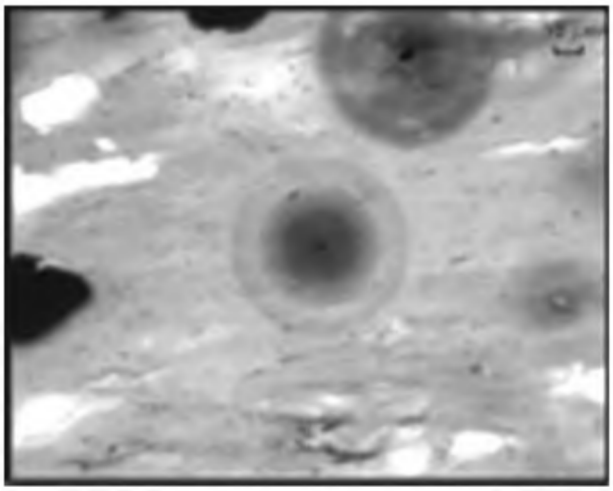

Figure 4. Photomicrograph of a typical radioactive halo in chlorite surrounding uraninite showing concentric rings of radiation damage. At least four damaged aureoles can be identified. The radiocentre diameter is 1.87 μm and the radii of the four rings are 31.9 , 21.9, 18.1 and 15.0 μm from the outermost to the innermost ring. See Table 1 and text for discussion.

observation is in accordance with field observation, where it was found that quartz-sericite schists are generally not mineralized and mark the limit of mineralized zones in Turamdih.

In thin section, the radius of radiation damage is a function of the nature of radiation source, the surrounding medium, the size of the radiocentre and the section of the damaged sphere. Theoretically, the best characteristic radius (maximum radius) of radiation damage would be represented in the diametral section and when the radiocentre is infinitely small. In the present study, for quantitative characterization, radiohalos with tiny (1–2 μm) radiocentres were chosen and measurements were taken on the plane where the radiocentres were focused. Radiocentres lying on the surface or near the surface of the thin section were preferred. After capturing images of such radiohalos, measurements were done using image analysing software (LEICA–QWIN). For individual rings in a radiohalo, 4–5 radii were measured and the mean of these measurements was taken to represent the radius of that particular ring in that radiohalo.

At least four clear rings are discernible in many halos. Typical concentric radiohalo rings in chlorite from the Turamdih U-ore are shown in Figure 4. Schematic diagram of ^{238}U radiohalo pattern based on penetration depths of alpha in air[2] is shown in Figure 5 *a*. Figure 5 *b* shows the line drawing of different rings of the radiohalo from Figure 4. A fifth inner ring was suspected under higher magnification. However, the boundary of this ring is not clear and hence it is marked by a dotted curve. Statistical data for this curve could not be obtained because of unclear boundary. Comparison of the Figure 5 *a* and *b* reveals that there is excellent matching between the theoretical radiohalo patterns of ^{238}U based on air alpha ranges (Figure 5 *a*) and those found in chlorite from Turamdih (Figure 5 *b*). Ring diameters were measured from fifty such radiohalos where ring-boundaries are clearly visible and relevant data are given in Table 1. The mean radii of the four rings from outermost to innermost are 32.4, 22.0, 18.3 and 15.2 μm. These data compare well with the theoretically calculated ring diameters in biotite[4], ^{4}He-induced coloration bands in biotite[2] and also with the observed ring diameters in natural biotite[2,3]. For comparison, these data are given in Table 1. The four rings (marked by solid curves in Figure 5 *b* and data in Table 1) from outermost to innermost, correspond to the penetration depths of alpha particles emitted by ^{214}Po (outermost ring), ^{218}Po, ^{210}Po/^{222}Rn, and ^{226}Ra/^{234}U/^{230}Th. The gaseous ^{222}Rn can escape the micro-system related to each radiohalo through favourable conduits in the form of micro-fracture and cleavage. However, the presence of radiohalos related to the daughters (^{218}Po ^{214}Po, ^{210}Po) of ^{222}Rn indicates that radon loss was not pervasive, though part of it can escape the system. The suspected fifth ring, mentioned earlier, may correspond to ^{238}U (innermost ring with dotted boundary in Figure 5 *b*). Strong radiation damage caused by ^{234}U/^{226}Rn/^{230}Th resulting in dark discoloration surrounding the radiocentre might have smeared the fifth ring. The ring pattern as found in the present study can thus be assigned to the chain decay of ^{238}U.

This study provides petrographic documentation of radiohalo patterns in chlorite caused by the decay chain of ^{238}U. It has shown that the damage pattern and penetration depths of α-particles are similar to those found in biotite. To the best of the author's knowledge, such studies are not available on natural chlorites, at least from India. The observational data presented here will add to the existing data and this study offers an opportunity for future research to characterize and understand the nature of radiation damages in sheet silicates in general and chlorite in particular, using modern techniques like laser-Raman spectroscopy, optical absorption micro-spectro-

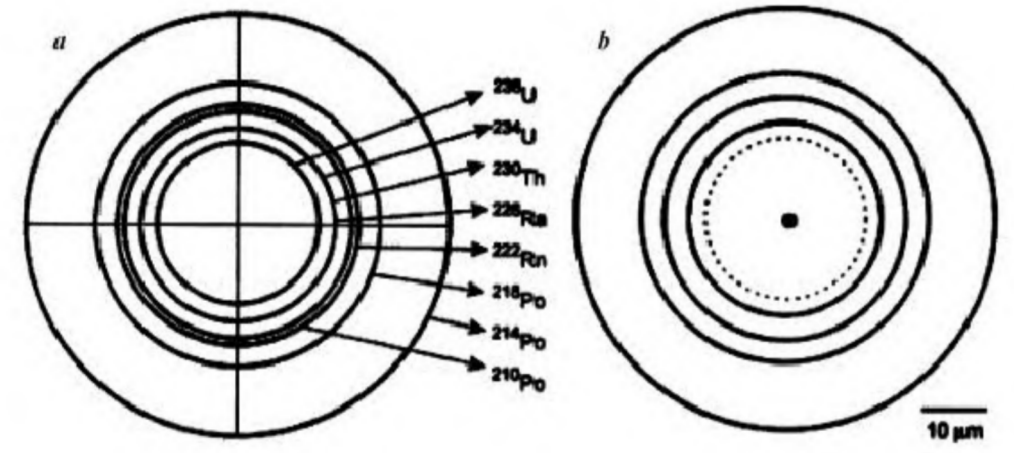

Figure 5. ***a***, Schematic diagram of ring pattern expected in a typical radioactive halo associated with the chain decay of ^{238}U based on the energies of α-particles emitted by different daughters of the ^{238}U-decay chain. Modified after Gentry[2]. ***b***, Line drawing of different concentric rings as presented in Figure 4. A fifth ring is suspected and is shown as dotted circle. Note the excellent matching of patterns in Figure 5 *a* and *b*. Also note the corresponding α-emitters.

scopy, high-resolution transmission electron microscopy, etc. Preliminary investigation in this direction is currently underway. It is also interesting to note that although the rock is highly deformed, none of the radiohalos observed in the present study shows any signature of deformation of the host mineral. This is a clear indication of the post-kinematic origin of the radiohalos. Trails of radiocentres with their characteristic radiohalos along foliation planes in tandem with the undeformed nature of the radiohalos are also possible indications of the post-kinematic origin for the radiocentres. Possible leaching of uranium by later processes may have important implications in U–Pb geochronological investigation.

1. Wang, L. M., Wang, S. X., Gong, W. L. and Ewing, R. C., Temperature dependence of Kr ion-induced amorphization of mica minerals. *Nucl. Instrum. Methods Phys. Res. B*, 1998, **141**, 501–508.
2. Gentry, R. V., Radiohalos in radiochronological and cosmological perspective. *Science*, 1974, **184**, 62–66.
3. Rankama, K., *Isotope Geology*, Pergamon Press, London, 1950, p. 535.
4. Nasdala, L., Wenzel, M., Andrut, M., Wirth, R. and Blaum, P., The nature of radiohaloes in biotite. Experimental studies and modeling. *Amn. Mineral.*, 2001, **86**, 498–512.
5. Moazed, C., Overbey, R. and Spector, R. M., Precise determination of critical features of radiohalo-type coloration of biotite. *Nature*, 1975, **258**, 315–317.
6. Moazed, C., Overbey, R. and Spector, R. M., Alpha-induced coloration reversal in biotite. *Nature*, 1977, **267**, 818–819.
7. Odom, L. A. and Rink, W. J., Giant radiation-induced colour halos in quartz: solution to a riddle. *Science*, 1989, **246**, 107–109.
8. Durrance, E. M., Radioactivity in *Geology. Principles and Applications*, Ellis Horwood Limited, Chichester, 1986, p. 441.
9. Chakoumakos, B. C., Murakami, T., Lumpkin, G. R. and Ewing, R. C., Alpha-decay-induced fracturing in zircon: the transition from the crystalline to the metamict state. *Science*, 1987, **236**, 1556–1559.
10. Murakami, T., Chakoumakos, B. C., Ewing, R. C., Lumpkin, G. R. and Weber, W. J., Alpha-decay event damage in zircon. *Am. Mineral.*, 1991, **76**, 1510–1532.
11. Meldrum, A., Boatner, L. A., Weber, W. J. and Ewing, R. C., Radiation damage in zircon and monazite. *Geochim. Cosmochim. Acta*, 1998, **62**, 2509–2520.
12. Weber, W. J., Ewing, R. C. and Wang, L. M., The radiation induced crystalline to amorphous transition in zircon. *J. Mater. Res.*, **9**, 688–698.
13. Nasdala, L., Pidgeon, R. T. and Wolf, D., Heterogeneous metamictization of zircon on a microscale. *Geochim. Cosmochim. Acta*, 1996, **60**, 1091–1097.
14. Sarkar, S. C., Geology and Ore Mineralization of the Singhbhum Copper–Uranium Belt, Eastern India, Jadavpur University Press, Kolkata, 1984, p. 263.
15. Firestone, R. B. and Shirley, V. S., *Table of Isotopes*, Wiley, New York, 1996, vol. 2, C5–C6.

ACKNOWLEDGEMENTS. This work is funded by Centre of Advanced Studies, Department of Geological Sciences, Jadavpur University and by the Jadavpur University Research Grant. I thank Shri R. K. Gupta, Chairman and Managing Director, UCIL for permission to work in the Turamdih mines. Cooperation extended by Shri A. K. Sarangi, Shri D. M. Kolte and Shri D. K. Das, UCIL during fieldwork is acknowledged. Constructive criticism and suggestions from three anonymous referees have improved the manuscript significantly.

Received 18 December 2003; revised accepted 13 July 2004

Model studies of ocean bottom seismometer experiment for gas-hydrate exploration

P. Prasada Rao, Sanjeev Rajput, A. R. Sridhar, N. K. Thakur* and S. I. Reddi

Gas Hydrate Group, National Geophysical Research Institute, Hyderabad 500 007, India

We model the *P*- and *S*-wave velocities of gas hydrates and free gas-bearing sediments and obtain the travel-time response for suitably spaced ocean bottom seismometers (OBS) on sea floor. The different models are presented with contrasting physical properties which produce the travel time curves corresponding to the gas hydrate and free gas layers for varying source–receiver offsets of the OBS. 2D ray tracing is done on models of different configuration, i.e. varying depths of sea floor, gas hydrate zone (GHZ) and free gas zone (FGZ) with the same sediment thickness. The best representative model is selected for each case, which produces the significant ray bending and travel time skips at contrasting velocity horizons of gas hydrate-bearing sediment layer underlain by significantly low velocity layer of free gas. Our results indicate that OBS should be deployed at a minimum of 5 km separation for getting better travel time response for GHZ and FGZ. The present exercise aims to provide some synthetic data that could be useful in deriving a physical model and in planning future OBS experiments for gas-hydrate exploration.

OCEAN bottom seismometers (OBSs) are considered to be the most useful components for measuring *P*- and *S*-waves more accurately. High quality *P*- and *S*-wave data can be obtained from the OBSs to derive accurate subsurface geological information. Seismic techniques for remote detection of gas hydrates and associated shallow gas are getting focused on some basic observations from OBS studies. Quantification of gas-hydrate reserves and associated petro-physical properties could be estimated from the observed *P*- and *S*-wave data[1–4].

In ocean bottom seismics, the source or receiver is located at the seafloor. This procedure is more complex and hence expensive, but is significant in terms of data imaging and geological knowledge. OBS data are necessary to investigate layers that are deeper than bottom simulating reflector (BSR; from refracted waves) and to investigate the V_P and V_S structures[5,6]. In fact, low compressional velocity zone can be identified by the presence of free gas zone.

The important aspect of shear wave information in investigating gas hydrate-bearing sediments comes from a

*For correspondence. (e-mail: nkthakur@ngri.res.in)